On Triangulation Axes of Polygons*

Wolfgang Aigner† Franz Aurenhammer† Bert Jüttler‡

Abstract

We propose the *triangulation axis* as an alternative skeletal structure for a simple polygon P. This axis is a straight-line tree that can be interpreted as an anisotropic medial axis of P, where inscribed disks are line segments or triangles. The underlying triangulation that specifies the anisotropy can be varied, to adapt the axis so as to reflect predominant geometrical and topological features of P. Triangulation axes typically have much fewer edges and branchings than the Euclidean medial axis or the straight skeleton of P. Still, they retain important properties, as for example the reconstructability of P from its skeleton. Triangulation axes can be computed from their defining triangulations in $O(n)$ time. We investigate the effect of using several optimal triangulations for P. In particular, careful edge flipping in the constrained Delaunay triangulation leads, in $O(n \log n)$ overall time, to an axis competitive to 'high quality axes' requiring $\Theta(n^3)$ time for optimization via dynamic programming.

Keywords: Polygon; medial axis; anisotropic distance; triangulation; edge flipping

1 Introduction

Let P be a simply connected and closed polygon in the plane. A circular disk $D \subset P$ is called *maximal* (for P) if there is no other disk $D' \subset P$ with $D' \supset D$. The (Euclidean) *medial axis* of P is the set of centers of all maximal disks for P. This tree-like skeletal structure has proved a very useful descriptor of shape. Applications in diverse areas exist, and various construction algorithms have been proposed; see e.g., [2, 6, 8] and references therein.

The medial axis is a unique structure, as is the so-called *straight skeleton* [3, 8] of P, which is composed of angular bisectors of P and can serve as a piecewise-linear alternative to the medial axis. In certain applications, however, it is desirable to have some flexibility in designing a skeletal structure, be it for keeping its size small so as to reflect only the essential parts of P, or for the sake of stability with respect to slight boundary changes of P. Several attempts have been made to adapt and prune the medial axis and the straight skeleton accordingly; see Attali et al. [6] and Siddiqi and Pizer [16], and Tanase and Veltkamp [17], respectively.

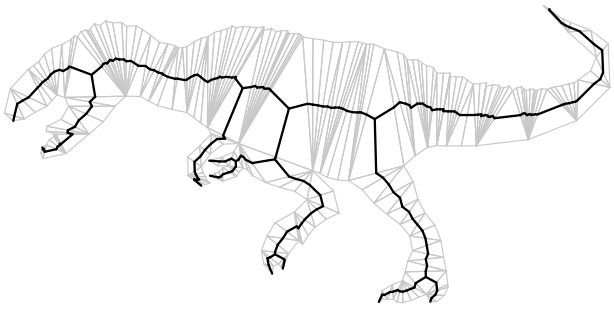

Figure 1: A triangulation axis of a simple polygon.

In the present note we propose a different idea, namely, of putting some anisotropy on the polygon P. Distances are measured differently at different locations within P, by varying the shape of the inscribed disks. (Anisotropic *Voronoi diagrams* where distances are measured individually from each defining point site have been introduced in Labelle and Shewchuk [14].) We divide the polygon P into triangles, and allot to each triangle a continuous family of unit disks, resulting from appropriately defined convex distance functions. (Voronoi diagrams for *convex distance functions* have been considered first in Chew and Drysdale [11].) The resulting skeleton is a straight-line tree resembling (but not equaling) the dual graph of the chosen triangulation of P. It always consists of fewer edges than the medial axis or the straight skeleton. When using the various known types of triangulation (e.g., constrained Delaunay [15, 10], minimum weight [13]), and also other triangulations optimal in different respects, we gain the needed flexibility, with the ultimate aim of defining a simple, stable, and characteristic skeletal axis structure for P.

In particular, we show that the constrained Delaunay triangulation of P, when post-processed by a small number of edge flips based on visibility within P, leads to satisfactory results: The empty-circle property ensures some closeness to the medial axis, and flipping has the effect of pruning away unim-

*Supported by ESF Programme EuroGIGA-Voronoi

†Institute for Theoretical Computer Science, Graz University of Technology, Austria, {waigner,auren}@igi.tugraz.at

‡Institute of Applied Geometry, Johannes Kepler University Linz, Austria, Bert.Juettler@jku.at

portant features. Several $O(n \log n)$ construction algorithms are available for this triangulation [8], so the new skeleton is fast and easier to compute than the medial axis or the straight skeleton.

A preliminary version of this work appeared in [4].

2 Triangulation axis

A *triangulation* T of a simple polygon P is a partition of P into triangles whose vertices are all from P. Let P have n vertices. We will assume $n \geq 4$ throughout, so that T contains at least one diagonal of P. To define what we will call the *triangulation axis*, $M_T(P)$, *of* P *and* T, the triangles which constitute T are categorized into three types: *ear* triangles, *link* triangles, and *branch* triangles – having one, two, or three sides that are diagonals of P, respectively; see Figure 2.

Depending on its type, a triangle Δ contributes a specific part to $M_T(P)$. If Δ is an ear triangle, then its axis part is the line segment that connects the midpoint of its unique bounding diagonal d of P to the vertex of Δ opposite to d. If Δ is a link triangle, then it contributes to $M_T(P)$ the line segment connecting the midpoints of the two bounding diagonals of P. Finally, if Δ is a branch triangle, then the three line segments that connect its side midpoints to the centroid[1] of Δ are taken. See Figure 2 again, where the individual axis parts are drawn in bold lines.

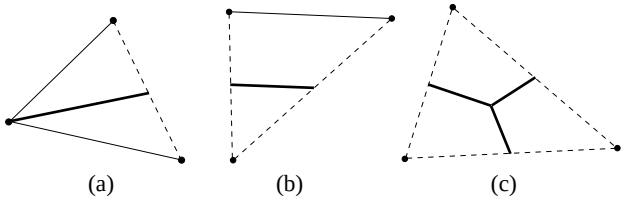

Figure 2: Triangle types: (a) ear triangle, (b) link triangle, and (c) branch triangle. Diagonals of P are drawn in dashed style, and triangulation axis parts in bold style.

The triangulation axis $M_T(P)$ is now defined as the geometric graph that has the aforementioned line segments as its edges and their endpoints as its vertices. $M_T(P)$ is a (straight-line) tree, as can be shown by an easy induction argument.

A particular triangulation axis of a polygon is depicted in Figure 1. Observe that link triangles (which typically constitute the majority in T) give rise to homothetic copies of P's boundary parts in the axis.

Indeed, $M_T(P)$ can be interpreted as an *anisotropic medial axis* of P. When suitable convex unit disks are used, the centroids of all possible *maximal* inscribed disks for P (as defined in Section 1) will delineate the triangulation axis. This is made explicit in Figure 3. Maximal disks for ear triangles and link triangles are just line segments of varying slopes. These line segments are parallel to the unique bounding diagonal for an ear triangle, see (a), and fan out from a vertex for a link triangle, see (b). Maximal disks for a branch triangle are of triangular shape, see (c), based on a particular side of the branch triangle and having one vertex on the respective median line. Note that maximal disks (and thus the anisotropy they exert) change continuously when their centers are moved along $M_T(P)$.

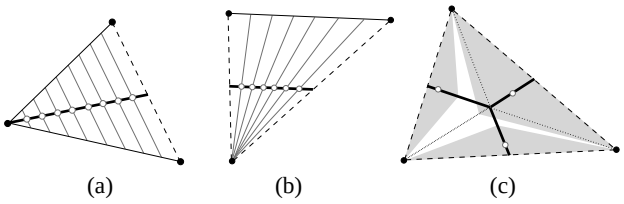

Figure 3: Maximal disks for the anisotropic convex distance function within (a) an ear triangle, (b) a link triangle, and (c) a branch triangle. White dots mark the centers (centroids) of the shown disks.

Triangulation axes are quite natural skeletal structures for polygons, though as far as is known to the authors, they did not receive much attention in the literature. We found recent mention of a triangulation axis in Wang [18] for GIS applications, who refers to Ai and van Oosterom [1] for earlier use. No systematic study of $M_T(P)$ has been provided though, and only the constrained Delaunay triangulation [10] of P has been used for T. In the following sections, we will elaborate on some structural and algorithmic properties of triangulation axes, and give some experimental results that reflect the behavior of this structure in dependency of the underlying polygon triangulation.

3 Basic properties

A nice feature of triangulation axes is their small combinatorial size.

Lemma 1 *Any triangulation axis of a simple polygon P with n vertices has between $n-2$ and $2n-6$ edges.*

Proof. Each triangulation T of P has the same number of triangles, $n-2$. Ear triangles and link triangles yield 1 edge of $M_T(P)$ each, whereas branch triangles contribute 3 edges. The number of edges of $M_T(P)$ thus is $n-2+2b$, with b counting the branch triangles of T. Moreover, we have $0 \leq b \leq \frac{n}{2} - 2$, the upper bound stemming from the fact that T has $b+2$ ear triangles, so that $(b+2)+b \leq n-2$. The claimed bounds follow by simple arithmetic. □

[1] Instead of the centroid, a different suitable point in Δ might be chosen; see Section 6.

In comparison, the medial axis of P consists of $2(n+r)-3$ edges [16], r of which are parabolically curved (one for each of the r reflex vertices of P), and the straight skeleton of P consists of $2n-3$ straight edges [3].

A desired property of skeletal axes is the ability of restoring the polygon P from its axis. Both the medial axis and the straight skeleton share this property; see [16] and [3], respectively. However, distances from the axis edges to the boundary of P have to be stored, in addition. (For the medial axis, this amounts to store the radii of certain maximal disks; the augmented structure is commonly called the *medial axis transform* of a polygon.)

Triangulation axes are even more well-behaved in this respect. Storing an additional bit for certain edges is sufficient to guarantee a unique reconstruction of P, except in the special case where the axis does not branch at all (and is just a path). In that case, the distance to a single non-ear vertex of P has to be remembered in addition.

Lemma 2 *Given any of its triangulation axes (which is not a path), a simple polygon P can be reconstructed in $O(n)$ time, provided at most $n-4$ extra bits are stored.*

Proof. We reconstruct P (more precisely, its underlying triangulation) triangle by triangle. Note first that triangle types can be recognized from the axis parts they yield. Actually, any branch triangle Δ is reconstructable uniquely, because Δ is just a rotated copy of the triangle formed by the midpoints of Δ's sides, in doubled size. As we have assumed that the axis contains branchings, there exists at least one branch triangle. If the neighbored triangle is an ear triangle, its reconstruction is trivial, too. In the case of a link triangle, we have two choices of following P's boundary in a way parallel to the respective axis edge; see Figure 4. Storing a 'left/right' bit is sufficient in that case. In total, at most $n-4$ bits are needed, because any triangulation of P has $n-2$ triangles, and at least 2 among them have to be ear triangles. □

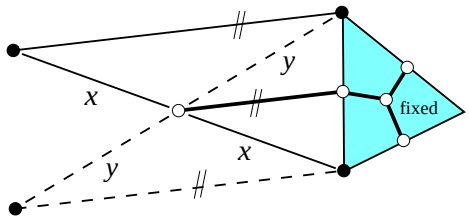

Figure 4: Two possible link triangles to continue.

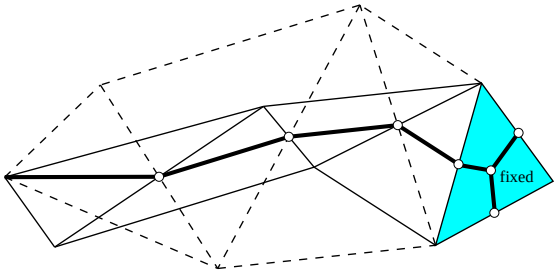

Figure 5: The empty-circle property does not help for restoring a polygon from its constrained Delaunay triangulation axis. For both polygons (shown in full lines and dashed lines, respectively) this axis is the same.

By contrast, the medial axis of P has $n+r-2$ inner vertices, for each we need to store the radius of the maximal disk centered there.

Without extra information, the polygon reconstruction from a triangulation axis is ambiguous, in general. This is even true when the triangulation is known to be *constrained Delaunay* in advance; see Figure 5. This particular triangulation of P is defined to consist of all diagonals $\overline{uv}$ of P with the following property [15, 10]: There exists some circle passing through u and v but enclosing no vertex w of P such that $\overline{uw}$ and $\overline{vw}$ are both diagonals of P.

The next lemma indicates that triangulation axes tend to describe the topology of a polygon more compactly than the medial axis.

Lemma 3 *For no triangulation T, $M_T(P)$ has more branchings than the medial axis of P.*

Proof. Both axes are trees whose leaves have to be vertices of P. Each convex vertex v of P is a leaf of the medial axis, whereas v is a leaf of $M_T(P)$ only if T contains an ear triangle at v. Reflex vertices of P cannot be leaves in either axis. It remains to observe that the number of branchings in any tree is exactly 2 less than the number of its leaves. □

4 Choice of triangulation

The geometry and topology of the triangulation axis $M_T(P)$ strongly depend on the choice of the underlying triangulation T. We will discuss some prominent representatives for T and some of their variations in the sequel.

The *constrained Delaunay triangulation* of P seems a good choice at first glance, as it tends to avoid edges at flat convex vertices of P, by its empty circle property. However (and similar to the notorious problem with the medial axis of P), still various small and unimportant features are reflected by this 'Delaunay

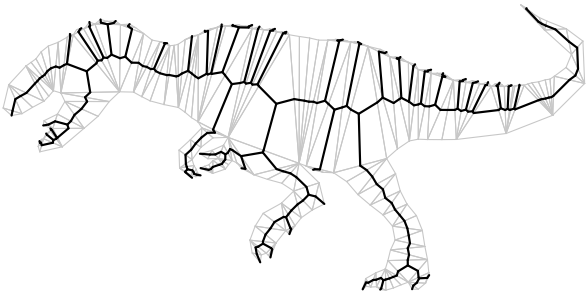

Figure 6: Constrained Delaunay triangulation.

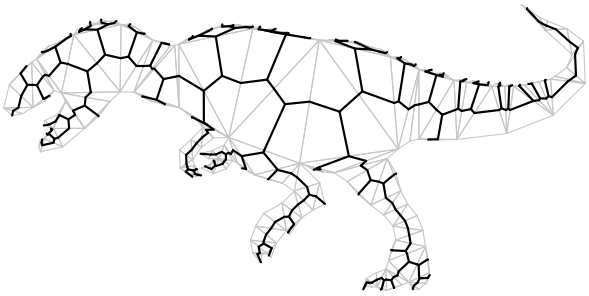

Figure 7: Minimum weight triangulation.

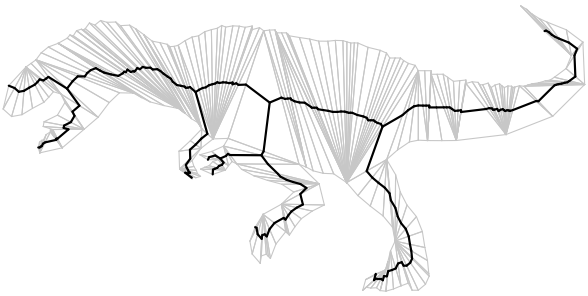

Figure 8: Minimum axis length.

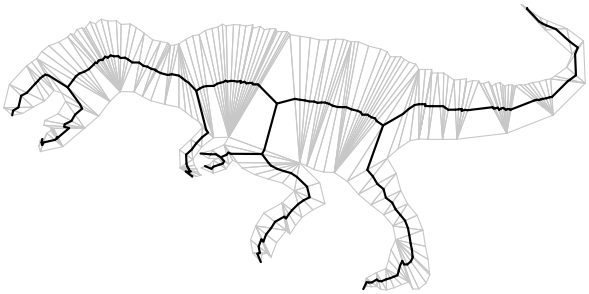

Figure 9: Minimum weight triangulation where branch triangles are expensive.

axis' of P; see Figure 6. Also, it lacks optimization properties like maximizing angles or minimizing lengths, as can be shown by examples. An advantage is the low construction time of $O(n \log n)$; see e.g., [10].

The *minimum-weight triangulation* of P, which is defined to minimize the sum of edge lengths [13], appears a promising candidate as well: A 'short' triangulation might have edges nicely aligned within P. Unfortunately, small length implies many branch triangles, as these triangles are capable of covering much polygon area, leaving less area (and thus edge length) for the most frequent type of axis edges, the link edges; see Figure 7. However, weighting each branch triangle by k times its perimeter, for some large constant k (rather than using $k = 1$ for all triangles, which gives the minimum-weight triangulation) yields quite satisfactory results; see Figure 9. Note that the type of each triangle can be read off from the vertices of P it uses. The runtime of $\Theta(n^3)$ that results from dynamic programming [13] is a clear disadvantage of these (and the following) types of triangulation, though.

The weight of a triangle can also be chosen as the length of the axis part it yields. This *minimum length triangulation axis*, see Figure 8, looks comparable to the axis in Figure 9, which was slightly better, however, as no inadequate paths close to leaves do occur that stem from keeping the axis shortest possible. Another possibility is to minimize the number of branch triangles (by granting them weight 1, with the remaining triangles getting weight 0). The resulting axis also minimizes the number of leaves, hence maximizes the number of links. The optimal solution is highly ambiguous, though, and its ability of describing the polygon turned out to be inferior to the former choices for most instances. (Still, a good candidate is given by the modified minimum-weight triangulation, with the weight k of branch triangles being sufficiently large.)

The axes in Figure 8 and 9 nicely resemble the predominant features of the polygon's medial axis. Even if P is poorly sampled at narrow passages, the 'interesting parts' of $M_T(P)$ are geometrically not too far apart from the latter structure; see also Figure 10. In particular, $M_T(P)$ behaves better in such cases than

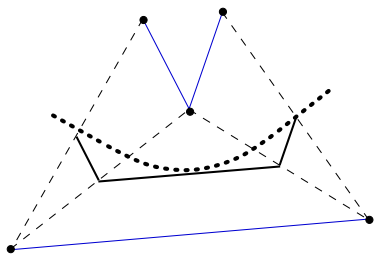

Figure 10: Medial axis deviation (dotted curve) from the triangulation axis (bold lines) within a link triangle.

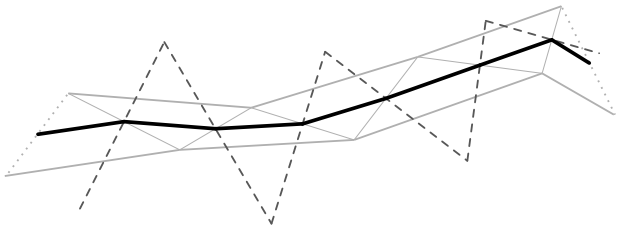

Figure 11: Triangulation axis (bold edges) and pruned Voronoi diagram (dashed edges).

an approximation by the (pruned) Voronoi diagram of P's vertices (a widely used linearization of the medial axis [16]), because such skeletons may exit and re-enter the polygon at several places, as Figure 11 illustrates.

The straight skeleton of P, in turn, is also no adequate linearization in general, because its inner nodes might get arbitrarily close to the boundary of P (instead of being 'centered') in the presence of sharp reflex polygon vertices; see Figure 12. This is due to the high speed of such vertices in the shrinking process which defines the straight skeleton [3]. A possible way out might be to weight the speed of the polygon edges individually to milden this undesirable effect, that is, to use a weighted straight skeleton [7] of P.

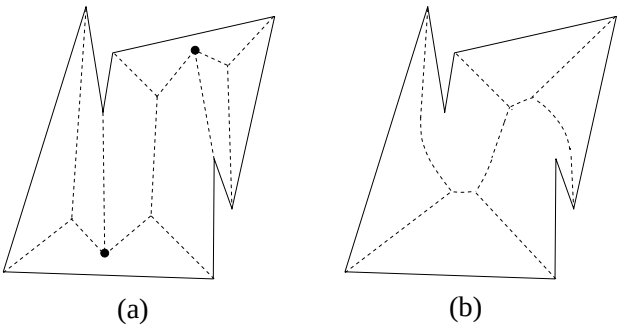

Figure 12: (a) Two straight skeleton nodes get close to the polygon boundary. This cannot happen for the medial axis (b) which by definition stays centered.

5 Edge flipping

Triangulation axes can be modified (and improved) gradually by *flipping edges* in their defining triangulation T of the input polygon P.

Let e be an edge of T but not of P, and assume that the two triangles of T adjacent to e form a convex quadrilateral Q. Flipping the edge e means replacing e by the other possible diagonal of Q. Note that the structure resulting from the flip is still a triangulation of P. It is well known that any two triangulations of P can be transformed into each other by a sequence of edge flips; see e.g. [12].

Our goal is to start with the constrained Delaunay triangulation of P (which has a low construction time, $O(n \log n)$), and to automatically prune away unwanted pieces of the Delaunay axis by well-chosen edge flips. A different pruning approach, based on removing certain axis parts *without* adapting its remaining edges is proposed in Wang [18].

Consult Figure 13. If the bottommost branch of the axis is considered unimportant (e.g., because of its short length) then it can be possibly removed, by destroying the shaded branch triangle and flipping in certain link triangles.

More precisely, define a *fibre* of the axis $M_T(P)$ as the unique path from a leaf u of $M_T(P)$ to the first branching point reached (if it exists). Let Δ be the respective branch triangle, and consider the vertex v of Δ lying opposite to u. If the part of P that corresponds to this fibre is entirely visible from v, then this part can be re-triangulated by repeatedly flipping in edges incident to v. Thereby Δ gets destroyed and no new branch triangles are created. That is, the fibre gets removed from the triangulation axis.

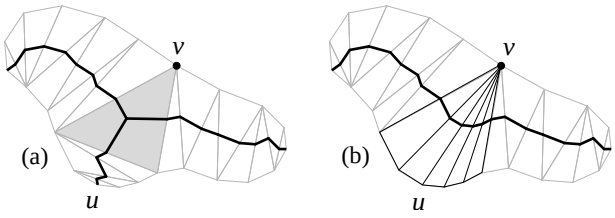

Figure 13: (a) The axis contains an unwanted branch. (b) Pruning the axis by flipping edges in the triangulation.

This 'clean up' step is now applied recursively, by establishing a hierarchy among the branch triangles Δ in T. Let us define the *level* of Δ as the minimum number k of branchings on a path in $M_T(P)$ from a leaf to Δ. Clearly, if Δ gives rise to a fibre then its level is 0. Observe further that we have $k = O(\log n)$; a maximum value of k is attained if T is a balanced binary tree. Pruning now proceeds in rounds, where in round i for $i \geq 1$ all branch triangles of level $i-1$ in T are considered. For each of them one fibre – if it exists in the axis for the current triangulation, and falls short of some length threshold – is pruned away by flipping.

Each round takes only $O(n)$ flips, because each created edge stays permanent in its level, and the total number of flips is therefore bounded by $O(n \log n)$. An overall runtime of $O(n \log n)$ is achieved, including the construction of the initial (constrained Delaunay) triangulation of P.

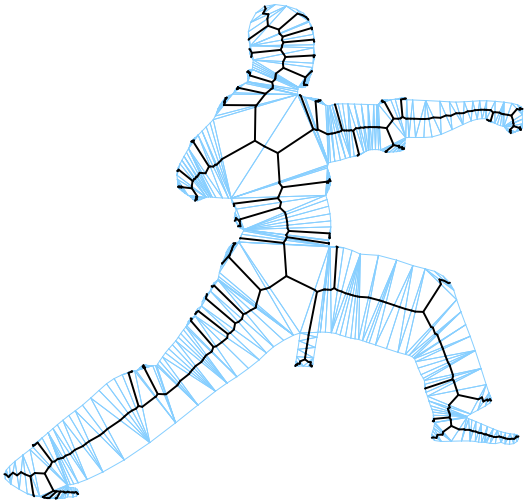

Figure 14: Delaunay axis.

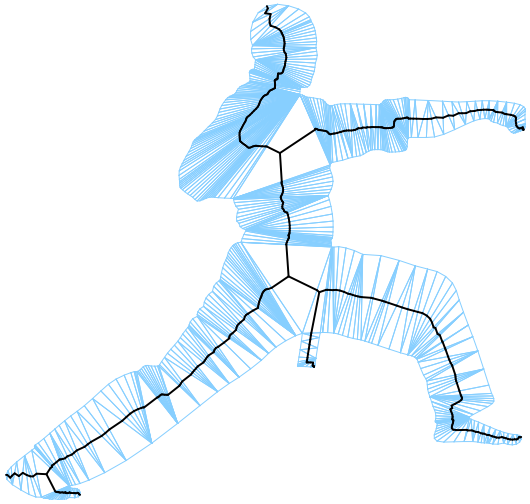

Figure 15: Recursively pruned Delaunay axis.

As a length threshold for a fibre, the *local feature size* [5] of its opposite vertex v (see Figure 13) can be taken. The local feature size of a point x on P's boundary is the distance from x to the closest point on the medial axis of P. For v, this distance can be (roughly) estimated by the side lengths of the respective branch triangle. Note that the choice of the length criterion does not affect the $O(n \log n)$ time bound for the axis construction.

The local feature size seems an appropriate indicator for 'unimportant' fibres, because it locally reflects the width of the polygon P. Informally speaking, if a fibre is not much longer than the local distance to the medial axis, then its contribution is not likely to be significant. On the other hand, long fibres which fulfill the visibility condition above are still likely to represent a significant branch of P, and thus should not be pruned away by flipping.

This simple heuristic is surprisingly effective. Figure 1 in Section 1, which has been computed in this way, shows an axis of quality comparable to the $\Theta(n^3)$ time optimal triangulation approaches in Figures 8 and 9. The many 'spurious' elements appearing in the unpruned constrained Delaunay axis (Figure 6) have been removed. The same improvement can be seen when comparing Figures 14 and 15. In particular, a *stable* skeleton has been constructed, whose topology will not change under small alterations of the shape boundary.

6 Discussion

We have introduced the triangulation axis of a polygon to computational geometry, with the intention to demonstrate its potential of being a simple, stable, and characteristic skeletal structure.

Several questions are raised by the investigations in the present note. The main issue, of course, is to find a fast and provably good method of adapting the underlying triangulation to the shape of the polygon. We have undertaken first steps towards this goal in Section 5.

A convergence result with respect to the medial axis would be desirable, if extraneaous vertices on P's boundary are allowed. Does a carefully pruned Delaunay axis of P, or a slight variant thereof, converge to the medial axis if boundary sampling gets arbitrarily fine (except within branch triangles, where we can replace axis parts accordingly)?

As a minor issue, choosing a reference point other than the centroid for a branch triangle Δ may improve the geometric quality of the triangulation axis. In principle, any point in Δ can be taken that changes continuously with Δ and that, when Δ is 'squeezed' to a line segment, converges to its midpoint. All properties described in Sections 2 and 3 then stay valid. Anisotropic convex distance functions still can be de-

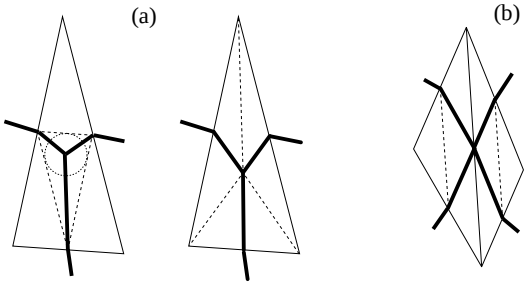

Figure 16: (a) Incenter of ∇ versus centroid of Δ. (b) Axis vertex of degree 4 that results from using Steiner points.

fined, and the reconstruction of the polygon is the same. In fact, the *incenter* (center of the inradius) of the triangle ∇ spanned by Δ's side midpoints gives slightly better results than the centroid. This point stays closer to the side midpoints, see Figure 16(a), which causes the resulting axis to 'wiggle' less. Taking the *Steiner point* [9] of ∇, which by definition minimizes the length of the axis part within Δ, is an option as well. Note that this point may coincide with a side midpoint of Δ, and give rise to an axis vertex of degree 4 if two branch triangles are adjacent; see Figure 16(b). We have used the better one of these branch points for each individual Δ in our computer-generated examples (Figures 1, 6-9, 14, and 15).

Let us mention at this place that taking just the *dual graph* of a polygon triangulation, which contains a single dual edge for each diagonal used, is a less convenient candidate for a skeleton. If not placed carefully, this graph might be far from being centered, and even may leave the polygon when drawn with straight-line edges.

The concept of triangulation axis is not restricted to simple polygons, but extends to polygonal regions with holes. The question arises whether there exists a meaningful generalization to three dimensions. A carefully defined triangulation axis of an interior-triangulated polytope might lead to a useful one-dimensional skeletal structure. (Computing the 1-skeleton of the 3D medial axis, or a linearization thereof, is quite elaborate [16].) The main obstacles faced are the existence of tetrahedrizations having size $\Theta(n^2)$, and the occurrence of cycles in their dual graph. On the other hand, flipping still works for tetrahedral partitions.

References

[1] T. Ai and P. van Oosterom. GAP-tree extensions based on skeletons. *Proc. 10th Int. Symposium on Advances in Spatial Data Handling*, Springer Verlag, 2002, 501–513.

[2] O. Aichholzer, W. Aigner, F. Aurenhammer, T. Hackl, B. Jüttler, and M. Rabl. Medial axis computation for planar free-form shapes. *Computer-Aided Design* 41 (2009), 339–349.

[3] O. Aichholzer, D. Alberts, F. Aurenhammer, and B. Gärtner. A novel type of skeleton for polygons. *Journal of Universal Computer Science* 1 (1995), 752–761.

[4] W. Aigner, F. Aurenhammer, and B. Jüttler. On triangulation axes of polygons. *Proc. 28th European Workshop on Computational Geometry*, 2012, 125–128.

[5] N. Amenta and M. Bern. Surface reconstruction by Voronoi filtering. *Discrete & Computational Geometry* 22 (1999), 481–504.

[6] D. Attali, J.-D. Boissonnat, and H. Edelsbrunner. Stability and computation of medial axes—a state-of-the-art report. *Mathematical Foundations of Scientific Visualization, Computer Graphics, and Massive Data Exploration*, T. Müller, B. Hamann, B. Russell (eds.), Springer Series on Mathematics and Visualization, 2008, 109–125.

[7] F. Aurenhammer. Weighted skeletons and fixed-share decomposition. *Computational Geometry: Theory and Applications* 40 (2007), 93–101.

[8] F. Aurenhammer, R. Klein, and D.T. Lee. *Voronoi Diagrams and Delaunay Triangulations*. World Scientific Publishing Company, Singapore, 2013.

[9] C. Bajaj. The algebraic degree of geometric optimization problems. *Discrete & Computational Geometry* 3 (1988), 177-191.

[10] L.P. Chew. Constrained Delaunay triangulations. *Algorithmica* 4 (1989), 97–108.

[11] L.P. Chew and R.L.S. Drysdale. Voronoi diagrams based on convex distance functions. *Proc. 1st Ann. ACM Symposium on Computational Geometry*, 1985, 235–244.

[12] J. De Loera, J. Rambau, and F. Santos. *Triangulations*. Algorithms and Computation in Mathematics Vol. 25, Springer Verlag, 2010.

[13] G.T. Klincsek. Minimal triangulations of polygonal domains. *Annals of Discrete Mathematics* 9 (1980), 121–123.

[14] F. Labelle and J.R. Shewchuk. Anisotropic Voronoi diagrams and guaranteed-quality anisotropic mesh generation. *Proc. 19th Ann. ACM Symposium on Computational Geometry*, 2003, 191–200.

[15] D.T. Lee and A.K. Lin. Generalized Delaunay triangulation for planar graphs. *Discrete & Computational Geometry* 1 (1986), 201–217.

[16] K. Siddiqi and S.M. Pizer. *Medial Representations. Mathematics, Algorithms, and Applications*. Springer Series on Computational Imaging and Vision 37, 2008.

[17] M. Tanase and R.C. Veltkamp. A straight skeleton approximating the medial axis. *Proc. 12th Ann. European Symposium on Algorithms*, Springer Lecture Notes in Computer Science 3221, 2004, 809–821.

[18] T. Wang. Extraction of optimal skeleton of polygon based on hierarchical analysis. In J. Zhang et al. (eds.), *Int. Archives of Photogrammetry, Remote Sensing, and Spatial Information Sciences*, 28-7/C4, 2009, 272–276.